

Zeitschrift: IABSE reports of the working commissions = Rapports des commissions de travail AIPC = IVBH Berichte der Arbeitskommissionen

Band: 11 (1971)

Artikel: Ultimate static strength and fatigue behaviour of longitudinally stiffened plate girders in bending

Autor: Maeda, Yukio

DOI: <https://doi.org/10.5169/seals-12067>

Nutzungsbedingungen

Die ETH-Bibliothek ist die Anbieterin der digitalisierten Zeitschriften auf E-Periodica. Sie besitzt keine Urheberrechte an den Zeitschriften und ist nicht verantwortlich für deren Inhalte. Die Rechte liegen in der Regel bei den Herausgebern beziehungsweise den externen Rechteinhabern. Das Veröffentlichen von Bildern in Print- und Online-Publikationen sowie auf Social Media-Kanälen oder Webseiten ist nur mit vorheriger Genehmigung der Rechteinhaber erlaubt. [Mehr erfahren](#)

Conditions d'utilisation

L'ETH Library est le fournisseur des revues numérisées. Elle ne détient aucun droit d'auteur sur les revues et n'est pas responsable de leur contenu. En règle générale, les droits sont détenus par les éditeurs ou les détenteurs de droits externes. La reproduction d'images dans des publications imprimées ou en ligne ainsi que sur des canaux de médias sociaux ou des sites web n'est autorisée qu'avec l'accord préalable des détenteurs des droits. [En savoir plus](#)

Terms of use

The ETH Library is the provider of the digitised journals. It does not own any copyrights to the journals and is not responsible for their content. The rights usually lie with the publishers or the external rights holders. Publishing images in print and online publications, as well as on social media channels or websites, is only permitted with the prior consent of the rights holders. [Find out more](#)

Download PDF: 12.12.2025

ETH-Bibliothek Zürich, E-Periodica, <https://www.e-periodica.ch>

Ultimate Static Strength and Fatigue Behavior of Longitudinally Stiffened Plate Girders in Bending

Résistance à la ruine statique et comportement à la fatigue des poutres à âme pleine fléchies, munies de raidisseurs longitudinaux

Statische Tragfähigkeit und Ermüdungsverhalten längsversteifter, biegebeanspruchter Vollwandträger

YUKIO MAEDA

Dr.-Eng.

Professor of Civil Engineering
Osaka University, Osaka, Japan

I. INTRODUCTION

This paper is intended to present a study on ultimate static strength and fatigue behavior of thin-walled deep plate girders. The present study is based on experiments conducted at Osaka University, Japan, on longitudinally stiffened large-size welded steel plate girders, aiming at their test panel in pure bending.

Firstly, static bending tests are carried out to examine the influence of initial web deflection, slenderness ratio of web, rigidity of longitudinal stiffener and hybrid combination of materials upon the behavior of test panel in pure bending of the plate girders. Secondly, fatigue tests are made to examine patterns of initiation of fatigue cracks in the panels in pure bending of the plate girders, subjected to repeated loads, and the influence of aspect ratio of the test panels, slenderness ratio of web and longitudinal stiffeners upon lateral deflections of the web in relation with the initiation of fatigue cracks.

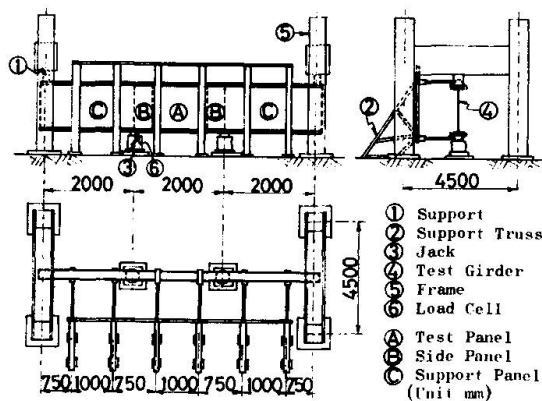
In this paper, the test results will be mainly described with discussions.

II. STATIC BENDING TESTS

1. Design of Test Girders

Design details of eight girders for the tests are given in Fig. 1 and Table 1.

Table 1. Dimensions of Test Panel of Static Test Girders



Girder No.	Size of Flange Comp.	Size of Flange Ten.	Size of Flange of Longl. Stiff.	t	b	b/t	a/b	$\frac{A_w}{A_f}$	$\frac{c}{d}$	$\frac{c_s}{d_s}$	$\frac{\gamma}{\delta^*}$
	(mm)	(mm)	(mm)	(mm)	(mm)						
B-1	200x13	200x13	—	4.50	1125	250	0.75	1.95	7.69	—	—
B-2	200x13	200x13	—	4.59	1349	294	0.75	2.38	7.69	—	—
B-3	200x13	200x13	60x5	4.72	901	191	0.75	1.56	7.69	12	3.65
B-4	200x13	20x13	65x5	4.56	1126	247	0.75	1.95	7.69	13	4.44
B-5	200x13	200x13	—	4.58	1351	295	0.75	2.38	7.69	14	4.72
B-6	200x10	200x10	50x50x6	4.65	902	194	0.75	1.56	6.00	12	3.84
B-7	200x10	200x10	50x50x6	4.51	1123	249	0.75	1.98	6.00	13	4.61
B-8	200x10	200x10	50x50x6	4.58	1351	295	0.75	2.41	6.00	14	4.72

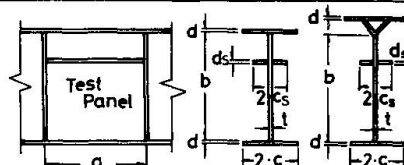


Fig. 1. Test Set-Up.

The large-size test girders are provided with a span length of 6.0 m and a web thickness of 4.5 mm, and consist of a test panel at the middle part, two supporting panels and two side panels, so that the girders can fail at the test panel subjected to pure bending. The girders are designed into three kinds of slenderness ratio b/t such as about 200 (Test Girders B-3 and -6), about 250 (Test Girders B-1, -4 and -7) and about 300 (Test Girders B-2, -5 and -8). The test girders B-6, -7 and -8 are provided with a Y-shape compression flange instead of a T-shape flange. All of

the test girders except B-1 and B-2 are stiffened by single double-sided longitudinal stiffener.

Thickness of the flange plates is designed to avoid a local buckling in plastic range of flange material. An actual rigidity J of the longitudinal stiffener is selected to be 3 to 5 times J^* , which expresses a theoretical rigidity required for an ideal stiffener by the linear theory of web buckling. These design rigidities were determined with the results of the author's preliminary tests¹⁾ at Osaka University. Furthermore, the preliminary tests have required that a connection of compression flange with transverse stiffeners and the one of longitudinal stiffener with transverse ones should be welded, to increase the ultimate strength. The girders were fabricated carefully by welding to make initial web deflections less than the web thickness, but a heating had to be applied to the weld part of flanges and stiffeners along the boundary of test panel, to satisfy the requirement for initial deflections of the girders except B-3 and B-6.

Steel material used for flange plates and angles is a corrosion resistant quenched and tempered alloy steel SMA58 (designated at JIS which is short for the Japanese Industrial Standards, with tensile strength $58 \sim 73 \text{ kg/mm}^2$). Steels used for webs and stiffeners are corrosion resistant high strength steel SMA50 (designated at JIS with tensile strength $50 \sim 62 \text{ kg/mm}^2$) and SS41 (designated at JIS with tensile strength $41 \sim 52 \text{ kg/mm}^2$, ordinary carbon steel), respectively. Coupon tension tests showed the following average yield stresses in kg/mm^2 , as 52.60 and 51.50 for 13 mm thick and 10 mm thick flange plates, respectively and 52.65 for flange angles and 50.80 for web plates.

2. Test Apparatus and Measurements

The test girders are simply supported at the upper ends below a shoe attached to two support frames fixed to a test floor, and loaded upward equally at a distance of 2.0 m from the both ends by means of two oil jacks of 200 tons capacity, so that the girder can be subjected to a constant pure bending moment between two loading points. The applied loads are recorded by two load cells of 200 tons capacity.

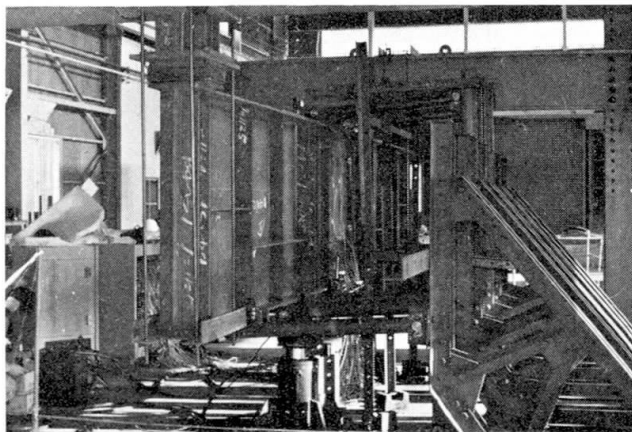


Fig. 2. Truss Frames against Lateral Buckling.

The flanges are restrained laterally by the use of six supporting truss frames rigidly connected to the test floor, as seen in Fig. 2. Lever arms of steel pipe with a diameter of 70 mm are pin-connected to the girder flanges at one end and to the truss frames at the other end, so as to allow free vertical and rotational movements, but restrict lateral movements of the flange.

Lateral deflections of web at the test panel before and during the test, are recorded by means of such a device made specially for the present tests, as shown in Fig. 3. Two steel square pipes of 50×50 in mm are fixed horizontally to two transverse stiffeners at the loading points. An alumi-

num angle bar to which dial gages are attached, will move along the square pipes which will act as a rail, and will be fixed by magnet stands when readings are made. Recordings of the web deflection are made by dial gages at points of 7×5 for the test girders B-1, -3, -4, -6 and 8×5 for B-2, -5, -8.

Each girder is instrumented with electrical resistance strain gages to measure strains on the transverse and longitudinal stiffeners as well as the flange and web plates, and readings are recorded by a digital automatic strain indicator. Vertical deflections of each girder and lateral and rotational movements of the flange at the test panel are recorded by dial gages.

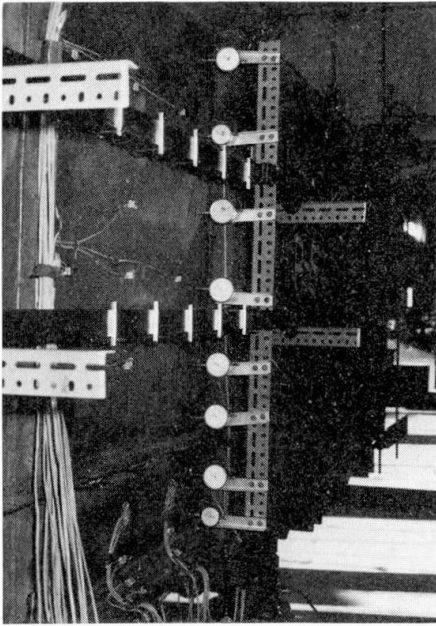


Fig. 3. Measurement of Web Deflections.

tic theory. Table 2 indicates that each value of P_u is larger than the corresponding value of P_{cr} for all of the girders, and that all of the values of P_u

Table 2. Theoretical Critical Loads and Observed Ultimate Load (in Ton)

Test Girder	P_{cr}	P_y	P_p	P_u
B-1	29.0	198.0	226.8	175.0
B-2	26.0	248.8	289.1	210.0
B-3	143.0	151.0	170.2	175.0
B-4	136.1	198.0	226.8	210.0
B-5	119.6	248.8	289.1	265.0
B-6	152.3	158.2	171.9	185.0
B-7	144.4	205.3	227.9	230.0
B-8	126.8	256.3	289.7	280.0

failure modes of the girders B-2, -5, -7 and -8 are demonstrated in (a), (b), (c) and (d) of Fig.4, respectively. The critical slenderness ratio of web against vertical buckling of the compression flange, when calculated with the equation

Table 3. Modes of Failure of Compression Flange

Test Girder	Ultimate Moment (t-m)	Mode of Failure
B-1	175	Torsional buckling
B-2	210	Vertical buckling
B-3	175	Torsional buckling with local buckling
B-4	210	Lateral buckling with local buckling
B-5	265	Lateral-torsional buckling with local buckling
B-6	185	Lateral buckling with local buckling
B-7	230	Lateral buckling with local buckling
B-8	280	Lateral buckling with local buckling

3. Test Results and Discussions

(1) Overall behavior of girders

It is noted that the girders which have a hybrid feature, showed a more rapid progress of deformation approaching to failure near the ultimate load than the one observed for the non-hybrid girders at the author's preliminary tests¹⁾. This observation could be explained by the facts that the compression flange had acted as one of the frame members to restrain strains in a web up to the first yield of web material at its upper edge, and then, with a progress of yielding of the flange material, the web strains in plastic region began to flow rapidly released from restraint by the flange, and that, on the other hand, ductility of the material used for the flange is smaller.

(2) Failure modes and ultimate strength

Ultimate loads P_u for each girder are given in terms of the total failure load in Table 2 with theoretical loads of web buckling P_{cr} calculated from the linear theory, theoretical loads of compression flange yielding P_y and theoretical full-plastic loads P_p calculated from the simple plastic theory. Table 2 indicates that each value of P_u is larger than the corresponding value of P_{cr} for all of the girders, and that all of the values of P_u except for B-1 girder are larger than the corresponding ones of P_y , and furthermore the value of P_y for B-3 and B-7 girders is larger than even the one of P_p .

Stresses which the web plate cannot resist owing to its deformations, have been generally redistributed to the compression flange, although the stress redistribution at B-3 and B-6 girders of $b/t = 200$ was not remarkably observed. Therefore, it seems that the collapse of plate girders can be governed by a failure of flange in compression.

Recorded ultimate collapse moments and observed failure modes of the compression flange for each girder are shown in Table 3. For examples, the

given by Basler²⁾, is larger than that given for the web of each test girder. Also, Toprac's equation³⁾ shows for all of the test girders that critical stresses for the vertical buckling are smaller than those for the lateral buckling and the torsional buckling. Therefore, it follows that the vertical buckling may not occur theoretically for any of the test girders, but B-2 girder collapsed due to the vertical buckling of compression flange with 70 mm inward penetration into the web after yielding of the flange over its whole thickness. Because an increase of lateral deflec-

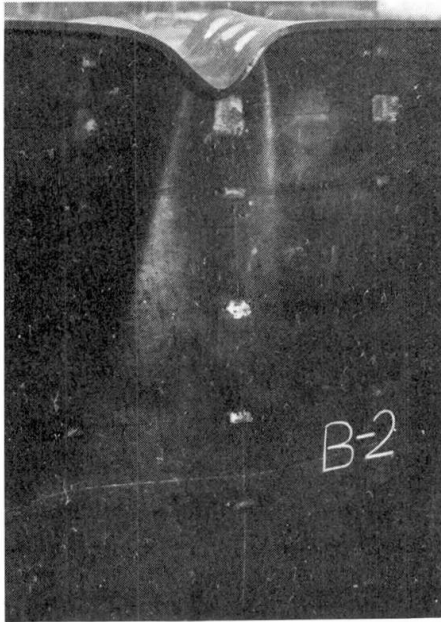


Fig. 4 (a)

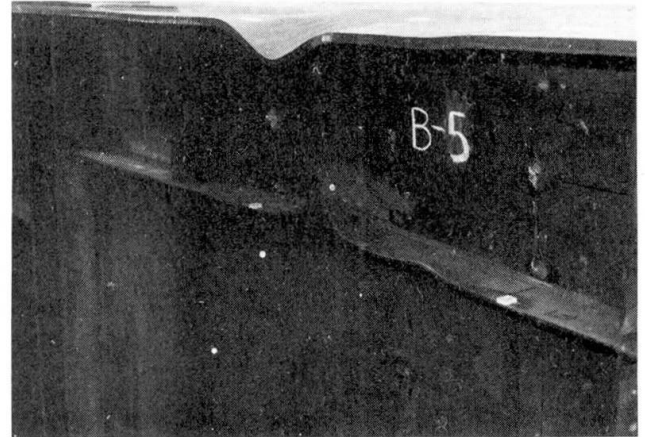


Fig. 4 (b)

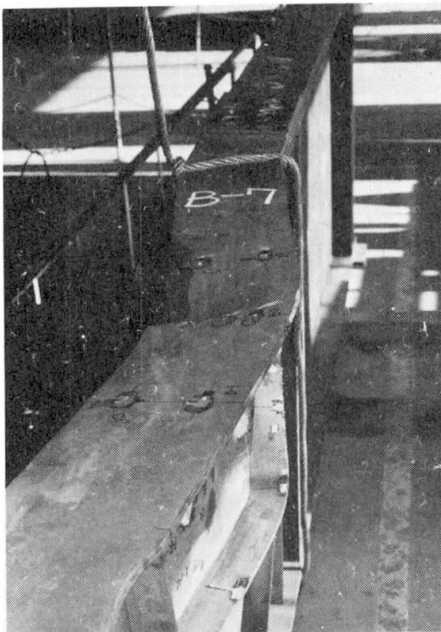


Fig. 4 (c)

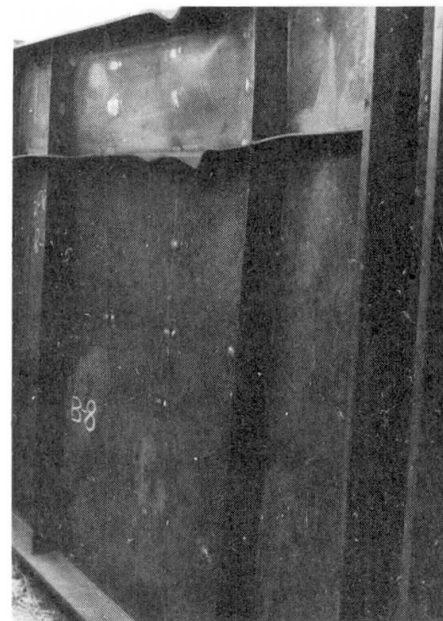


Fig. 4 (d)

Fig. 4. Examples of Failure Modes of Test Girders.

tions of the web which is not provided with a longitudinal stiffener, decreased greatly its vertical stiffness against the flange penetration.

Among B-2, -5 and -8 girders which have the same slenderness ratio of web 300, B-5 and B-8 did not show the vertical buckling, because the former is provided with the longitudinal stiffeners and the latter has a more stiff Y - shape flange. The test values of flange buckling for the test girders B-4, -5, -6, -7 and -8 which collapsed due to the lateral buckling, agreed fairly well with the calculated values by Basler's equation²). On the other hand, the test values of flange stress at the time of torsional flange buckling in the girders B-1 and B-3 verify well the

equation given by Basler ²⁾ and Haaijer ⁴⁾.

It is evident that a shape of compression flange influences greatly upon the pattern of flange buckling and the ultimate strength of girders. The sectional area of compression flanges is designed to be 260 cm^2 through all of the girders, but the shape is selected to be either T-shape or Y-shape. While vertical flexural rigidity and torsional rigidity of the Y-shaped flange are 15 times and 4 times the corresponding rigidity of the T-shaped flange, lateral flexural rigidity of the Y-shaped flange is 0.86 times that of the T-shaped one. In fact, B-6, -7 and -8 girders collapsed due to the lateral buckling of their Y-shaped flange. Furthermore, the girders with a Y-shaped flange showed a larger ultimate load than the girders with a T-shaped flange, compared under the slenderness ratio of web.

(3) Strain distributions in compression flange

The compression flange showed a uniform distribution of strains over its width up to $40\sim 60\%$ of the ultimate load, and afterwards exhibited in general a non-uniform distribution of strains due to lateral bending of the girder.

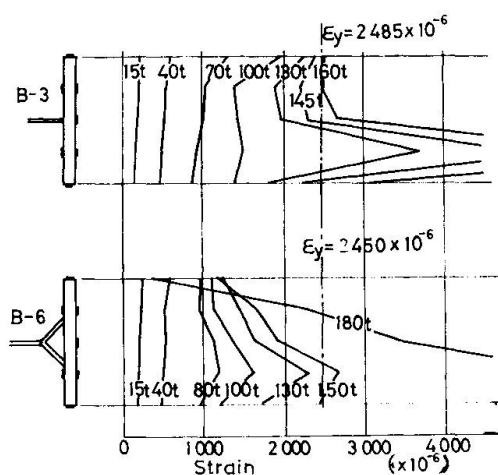


Fig. 5 shows the strain distribution in the compression flange of the girder B-3 which collapsed after the full yielding over its entire section and of the girder B-6 which corresponds to B-3 in the web slenderness ratio.

(4) Strain distributions on cross section of girder

Observation of strain distributions due to vertical bending reveals that, in the girders without longitudinal stiffener, redistribution of the web stresses to the compression flange develops accompanied by a large amount of movement of the neutral axis to the tension side, since lateral deflections of compressed part of the web increase from the initial stage of loading. Lateral deflections of the web of the girders provided with longitudinal stiffeners are restrained, so that especially the

Fig. 5. Strain Distributions in Compression Flange

girders B-3 and B-6 of $b/t = 200$ may demonstrate little the stress redistribution and their almost entire section acts effectively even at the final stage of loading, with only a little movement of the neutral axis. In the girders with b/t of 250 and 300, however, the web stresses are redistributed to the compression flange and the longitudinal stiffeners due to a decrease of resistance of the web against compression, because lateral deflections in a sub-panel in compression increase locally. Fig. 6 illustrates the observations for B-1 and B-7 girders.

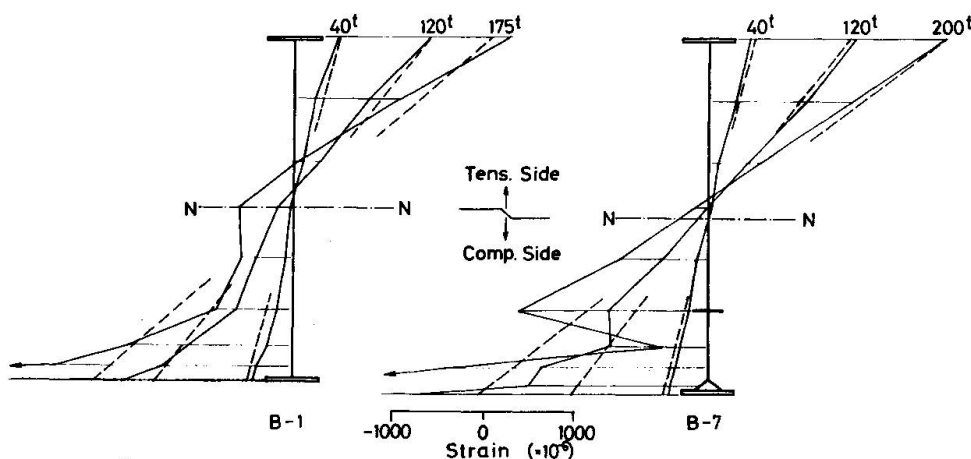


Fig. 6. Strain Distributions due to Bending

(5) Lateral deflection of web

Measurements showed that the maximum value of initial web deflections was $0.3\sim 0.7 \text{ t}$ for the girders of $b/t = 200$ and 300, and 1.3 t for the girder B-2 to 1.6 t for B-8 of $b/t = 300$, and that those values

were less than the limit $b/150$ specified by AWS Specifications⁵⁾. A decrease of strength due to these initial deflections was not clearly observed in the ultimate collapse load.

During loading, lateral deflections of the web of the girders not provided with longitudinal stiffeners, increased rapidly in the compressed part with an increase of load, to reach $3\sim 4$ t near the ultimate load. The lateral deflections of the web of the girders with longitudinal stiffeners increased gradually, but near the ultimate load increased abruptly, to reach to the maximum value of $0.5\sim 1.0$ t for the girders $b/t = 200$ and $1.0\sim 2.0$ t for $b/t = 250$ and 300 .

In general, the configuration of web deflections is the one of increased initial deflections, but the deflection curve of the girders without longitudinal stiffeners changed from an initial one with double curvatures to a final one with single curvature. Fig. 7 illustrates some measurements for the girders B-1, -4 and -7.

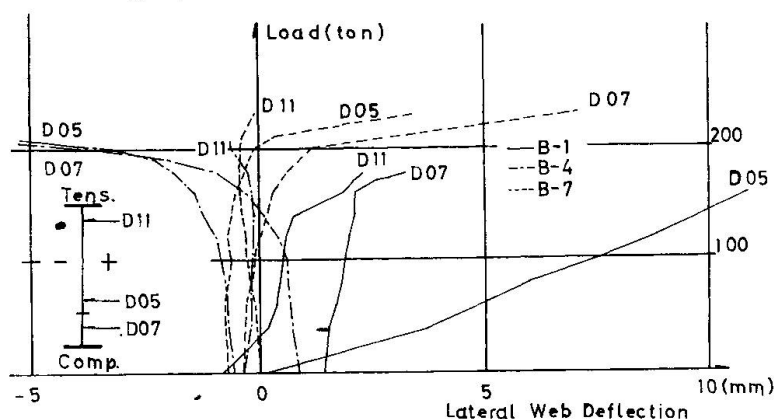


Fig. 7. Load versus Lateral Web Deflection

both stiffeners are welded together, so that the longitudinal stiffener behaved like a member of rigid frame for the sub-panel of the web, and its compressive strains increased with increasing loads, to exceed the yield strain of material near the ultimate load and then, to buckle with a similar mode with the flange.

On the other hand, transverse stiffeners showed a slight increase of strains with increasing loads, and finally reached to only about 500×10^{-6} .

(7) Effective width of web plate

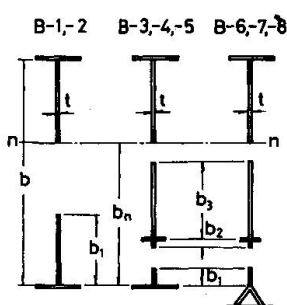
The flexural strains on a section at the center line of the test panel are shown for various loads in Fig. 6. The strains showed a nonlinear distribution due to an initial deflection of the web with an increase of load, and when loaded in the post buckled range of the web, a loss of effective width of the web resulted in moving of the neutral axis, a reduction of the effective sectional modulus and a corresponding increase of compressive strains.

Basler²⁾ gave 30 t for the effective width of web at the ultimate load for the girders without longitudinal stiffeners, but the present tests showed about 60 t for B-1 and about 48 t for B-2 as the effective width in the compressed side of the web. Table 4 gives the values of effective width, which are calculated by equating the resisting moment due to the compressive stress distribution about the

Girder No.	$\frac{b}{t}$	$\frac{b_1}{t}$	$\frac{b_2}{t}$	$\frac{b_3}{t}$	$\frac{b_e}{t}$	$\frac{b_n}{t}$	$\frac{b_e}{b_n}$
B-1	250	59.1	—	—	0.236	0.653	0.373
B-2	294	47.6	—	—	0.162	0.619	0.262
B-4	247	18.9	21.1	65.1	0.426	0.560	0.761
B-5	295	22.6	16.1	45.8	0.266	0.548	0.522
B-7	249	18.6	15.0	47.0	0.324	0.541	0.599
B-8	295	21.1	17.6	42.0	0.307	0.563	0.545

$$b_e = b_1 + b_2 + b_3$$

Table 4. Effective Width of Web



(6) Strains in longitudinal and transverse stiffeners

In the author's preliminary tests¹⁾ on large-size plate girders, an increase of strain of a longitudinal stiffener was hardly observed with increasing loads, because the longitudinal stiffeners not welded to transverse ones, were not restrained from their rotation with increasing deflections of the web. At the present tests, however, the

neutral axis to the moment of idealized stress distribution, taking into consideration a loss of the section at the compressed part of web or at each sub-panel in compression at the ultimate state. Since it could be observed that a full section of the girders B-3 and B-6 of $b/t = 200$ acted almost full effectively

without its loss, the values for those girders are excluded from Table 4. The Table indicates that the overall effective width is about 0.5~0.8 of the width in compression.

(8) Ultimate strength

The ultimate collapse load of plate girders will be governed by such parameters related to the pattern of buckling of their compression flange, as aspect ratio, web slenderness ratio, strength and rigidity of longitudinal stiffeners, sectional area ratio of web to flange, lateral and torsional rigidities of the compression flange, etc.

The ratio of test values of the ultimate moment to theoretical values of the full-plastic moment calculated from the simple plastic theory, is 0.77 for B-1, and 0.73 for B-2, but 1.03, 0.93 and 0.92 for B-3, -4 and -5, respectively and

1.08, 1.01 and 0.97 for B-6, -7 and -8, respectively. The girders provided with longitudinal stiffeners may resist against the ultimate moment almost close to the full - plastic moment.

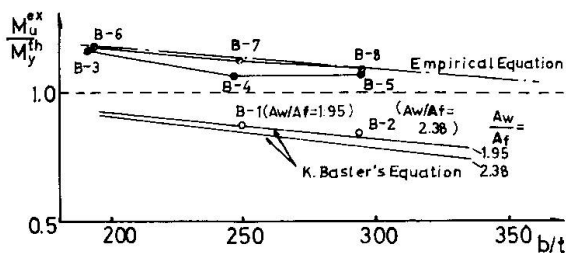


Fig. 8. Ultimate Moment versus Slenderness Ratio

stiffeners can carry, is about 1.2 times for $b/t = 250$ and 1.3 times for $b/t = 300$ as large as that for the girders with no longitudinal stiffener. It is seen that the ultimate loads calculated by the following equation which was proposed by Basler²⁾

$$\sigma_u = \sigma_y \left\{ 1 - 0.0005 \frac{A_w}{A_f} \cdot \left(\frac{b}{t} - 5.7 \sqrt{E/\sigma_y} \right) \right\}$$

are in good agreement with those obtained in the tests for the girders which are built-up with a hybrid combination of material.

It is furthermore recognized that the ultimate moments M_u^{ex} for the girders with longitudinal stiffeners are larger than the theoretical moments M_y^{th} correspondingly, and that M_u^{ex} for the girders with Y - shaped flange are larger than those for the girders with T - shaped flange. M_u^{ex} for the girders B-6, -7 and -8 will be expressed as an upper limit by the following experimental equation:

$$\frac{M_u^{\text{ex}}}{M_y^{\text{th}}} = -0.000796 \frac{b}{t} + 1.322,$$

which results in $M_u^{\text{ex}}/M_y^{\text{th}} = 1.0$ for $b/t = 405$.

III. FATIGUE TESTS

1. Design of Test Girders

Design details of six large-size welded test girders are illustrated in Fig.9 and dimensions of test panels are given in Table 5. Span length of the girders is 7.0 m, their web thickness is 3.2 mm, their web height is 80 cm or 96 cm, aspect ratio of the test panels is 0.75 or 1.0, and slenderness ratio of the web is 250 or 300. Half of the test girders are provided with single one-sided longitudinal stiffener in the test panels and the others are not provided with it. It should be noticed that the longitudinal stiffener is welded to transverse stiffeners, but the transverse stiffeners in the test panels are not welded to a flange in tension,

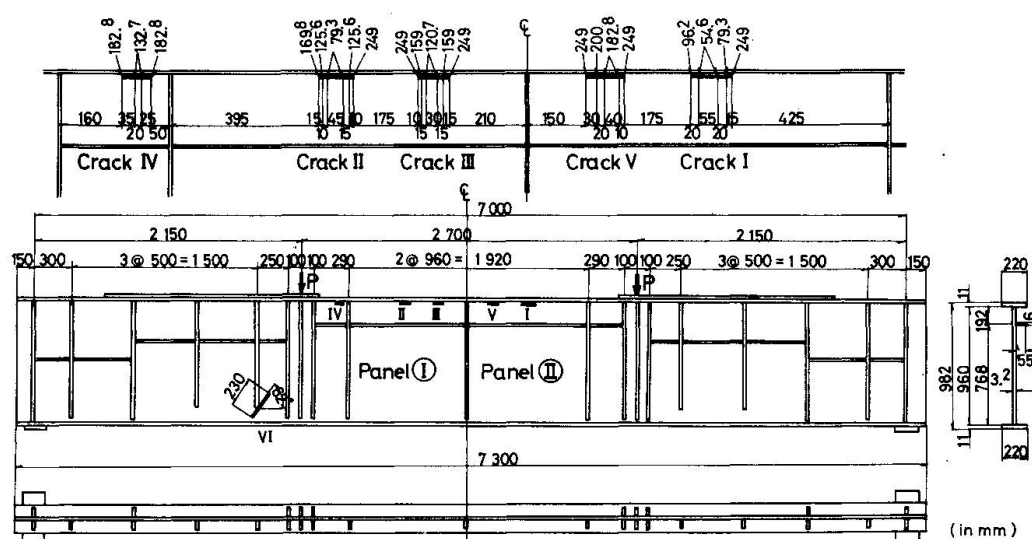


Fig. 9. Overall View and Fatigue Cracks of Girder F-5.

Table 5. Dimensions of Test Panels of Fatigue Test Girders

Girder No.	F-1	F-2	F-3	F-4	F-5	F-6
Size of Flanges (mm)	220x11	220x11	220x11	220x11	220x11	220x11
Depth of web, (b) (mm)	800	800	960	960	960	960
Thickness of web, (t) (mm)	3.2	3.2	3.2	3.2	3.2	3.2
Slenderness ratio, (b/t)	250	250	300	300	300	300
Spacing of Transverse Stiffeners, (a) (mm)	800	800	720	720	960	960
Aspect ratio, (a/b)	1.0	1.0	0.75	0.75	1.0	1.0
Number of Long. Stiff.	1	0	1	0	1	0
δ/δ^* for Long. Stiff.	4.28	—	5.30	—	5.83	—

but cut at 2 cm above the flange, to avoid a decrease of fatigue strength of the flange due to its welding to transverse stiffeners. The test girders are simply supported, and two concentrated equal loads P are applied to the girders downward at the distance of 2.15 m from each support. Therefore, the two test panels are subjected to a constant bending moment.

Steel material used for the flanges is a corrosion resistant high strength steel for welded structures SMA50 designated at JIS, and steel for the web and the stiffeners is respectively a high strength steel for ordinary structures SM50 and a carbon steel for welded structures SM41, designated at JIS.

2. Test Apparatus and Measurements

Repeated loads are applied with 285 cycles per minute by jacks of a Losenhausen -type universal fatigue testing machine, up to the number of cycles of $2 \sim 3 \times 10^6$, as seen in Fig. 10. The upper limit of one applied load is selected $20 \sim 22$ tons, up to which strains in the tension flange can keep a linear relationship with the load. The lower limit is selected $6 \sim 8$ tons so that the strains in the tension flange can be nearly equal to the dead load stress, which will occur at an actual bridge for which the test girders will be intended. Table 6 gives applied loads and stresses for each girder.

The girder is provided with truss-type frames against lateral buckling. At each number of loading such as 1×10^4 , 3×10^5 , 7×10^5 , 1×10^6 , 2×10^6 , the loads are lowered down to zero and measurements are carried out. For the test panels, stresses in flanges and web are recorded by strain indicators, and lateral deflections of the web are measured by dial gages. Also, vertical deflections at the span center and at $\frac{1}{4}$ span are measured by dial gages. An initiation of cracks due to fatigue is observed every number of loading of 3.5×10^4 .

3. Test Results and Discussions

(1) Fatigue cracks

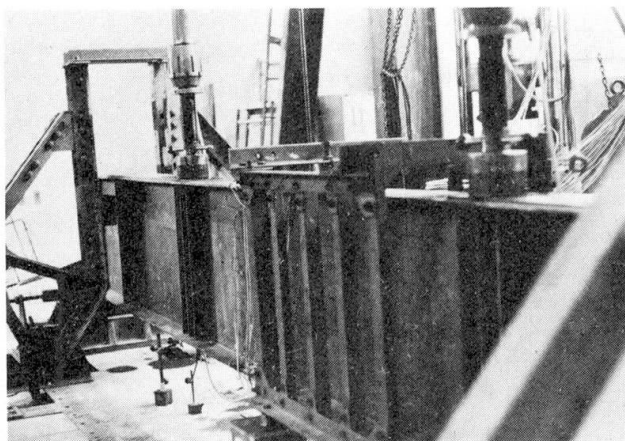


Fig. 10. Overall View of Test Set-Up.

Table 6. Applied Loads and Lower Flange Stresses

Girder No.	Applied Loads		Applied Stresses		
	P (ton)		σ (kg/cm^2)		
	P_{max}	P_{min}	σ_{max}	σ_{min}	$\sigma_{\text{max}} - \sigma_{\text{min}}$
F-1	21	8	2001	762	1239
F-2	20	8	1895	750	1137
F-3	22	6	1694	462	1232
F-4	20	6	1534	460	1074
F-5	21	6	1616	462	1154
F-6	20	6	1534	460	1074

Table 7. Initiation of Fatigue Cracks

Girder No.	Sequence of Cracks		Type of Cracks	Number of Cycles ($\times 10^4$)	Crack Length (mm)
	In Test Panels	Outside Test Panels			
F-1		I	BS-1	82.1	95
		II	BS-1	84.1	20
F-2	I	II	BM-1	40.5	125
			—	60.5	85
	III	V	BM-1	85.5	75
	IV		BM-1	104.0	75
			BS-1	162.8	140
F-3		I	BS-1	144.0	20
		II	—	150.0	130
F-4		I*	BS-1	56.6	30
		II	BS-1	154.9	40
F-5	I	IV*	BM-1	54.6	55
	II		BM-1	79.3	45
	III		BM-1	120.7	30
			BM-1	132.7	20
	V		BM-1	182.8	40
			BS-1	203.4	10
F-6	I	IV	BS-1	12.7	95
	II		BS-1	25.7	105
	III		BS-1	40.2	70
			BS-1	123.3	40



Fig. 11. Location of Cracks Type BM-1 in Girder F-5.

Toprac⁶⁾ divided the types of fatigue crack observed at his study on full-size hybrid girders under pure moment into three types, according to the location of cracks: Type BM-1, cracks found in the compression part of the web along the toe of fillet welds to connect web to flange; Type BM-2, cracks found in the web at the end of transverse stiffeners; and Type BM-3, cracks initiated in a tension flange.

Gurney⁷⁾ found at his study on fatigue strength of high tensile steel beams with transverse stiffeners under combined bending and shear, that Type BS-1 cracks among five types of fatigue cracks will be initiated prevalingly as the first crack. Type BS-1 cracks are found near the end of transverse stiffeners either in the heat affected zone of the web along the toe of the fillet welds or in the welds themselves, and propagate in the direction perpendicular to the tensile principal stress.

The initiation of cracks is summarized as shown in Table 7, where number of cycles and crack length at the time of crack finding are shown, and classifications are given according to the designation of Toprac and Gurney. In the table — mark means a crack not designated by the both, and * mark expresses a crack outside the test panels, but in the region of pure bending moment.

Figs. 9 and 11 shows initiations and propagations of cracks for the girder F-5. Fig. 12 illustrates a crack Type BM-1 found in the girder F-6. The test results indicate the following features:

- 1) Among the types of crack designated by Toprac and Gurney, only BM-1 and

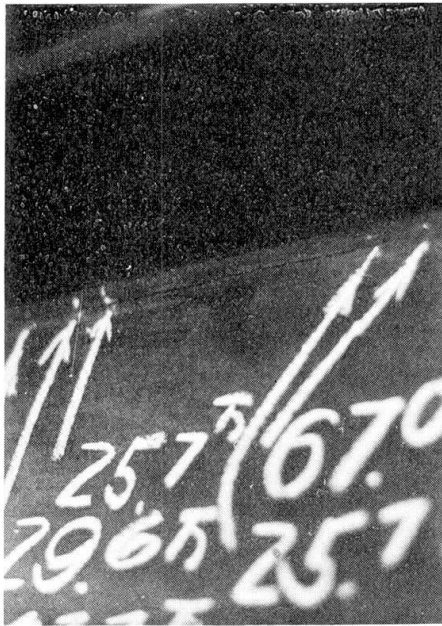


Fig. 12. Crack Type BM-1 in Girder F-6.

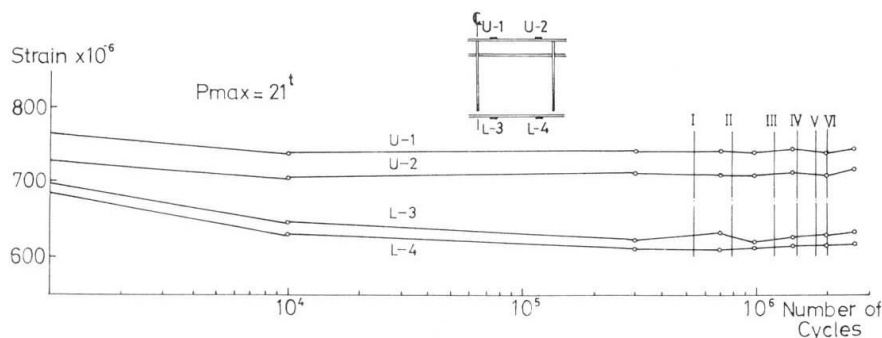


Fig. 13. Variation of Strains in Flanges of Girder F-5.

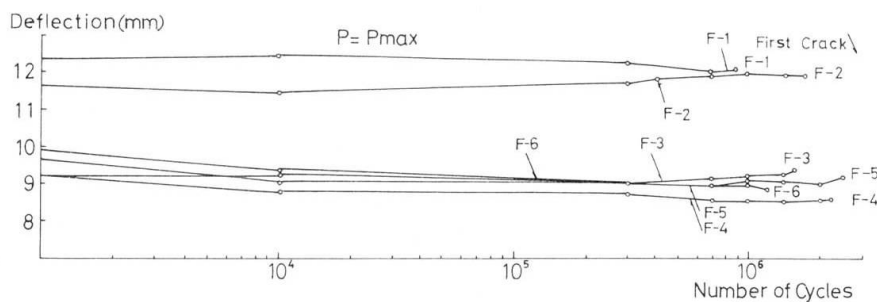


Fig. 14. Variation of Center Deflections for Girders.

ation of cracks Type BM-1 that the lateral deflection increased almost linearly with the repetition of loads.

Although large lateral deflections were observed in the tension part of web, these did not result in the initiation of crack Type BM-1, and after all the lateral deflections of part of web very near the compression flange have had a greater influence upon the initiation of Type BM-1, as seen in Fig. 15. This fact

BS-1 were found. Two cracks which did not belong to any type, were observed.

2) All of the cracks observed in the test panels are Type BM-1, which can be said to be a crack proper to thin-walled deep plate girders.

3) The cracks initiated outside the test panels are Type BM-1 or Type BS-1.

4) A decrease of flexural rigidity of the girder due to an initiation of Type BM-1 cracks in the test panels, do not have any distinct influences upon variations of strain in the flange and of deflection at the span center, as seen in Figs. 13 and 14, respectively.

(2) Lateral deflections of web and their influence on initiation of cracks Type BM-1

Since $b/t = 250$ and 300 are rather large and $t = 3.2$ mm is relatively so small, the maximum values of observed initial deflections of the web which are $0.62t \sim 1.9t$, are larger than those for the static test girders. The vertical distribution of initial web deflections at a section in the test panels consist of a double or triple curvature.

Configurations and amounts of the lateral deflections during loading are governed greatly by the state of initial deflections. With repetitions of loads, in general, the configuration of initial deflection moves upward and the deflections in the compression part of the web increase, while those in the tension part of the web decrease, with an increase of number of cycles. The web with a distribution of initial deflections in a single or double curvature showed larger lateral deflections, and in the case of triple curvature it showed smaller ones. It has been generally observed just before the initi-

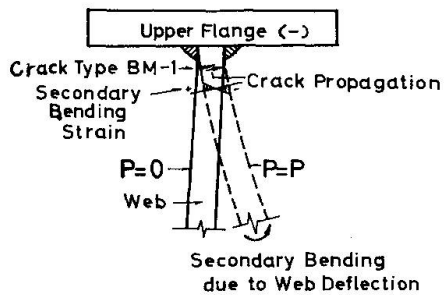


Fig. 15. Initiation of Crack Type BM-1 due to Secondary Bending of Web.

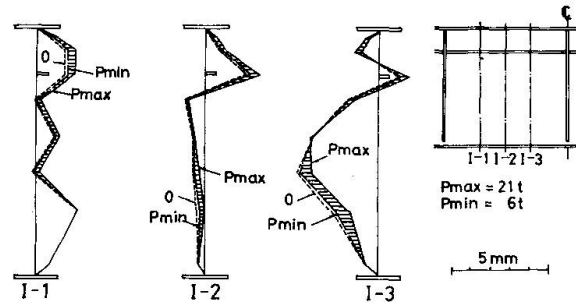


Fig. 17. Lateral Deflections of Web of Girder F-5.

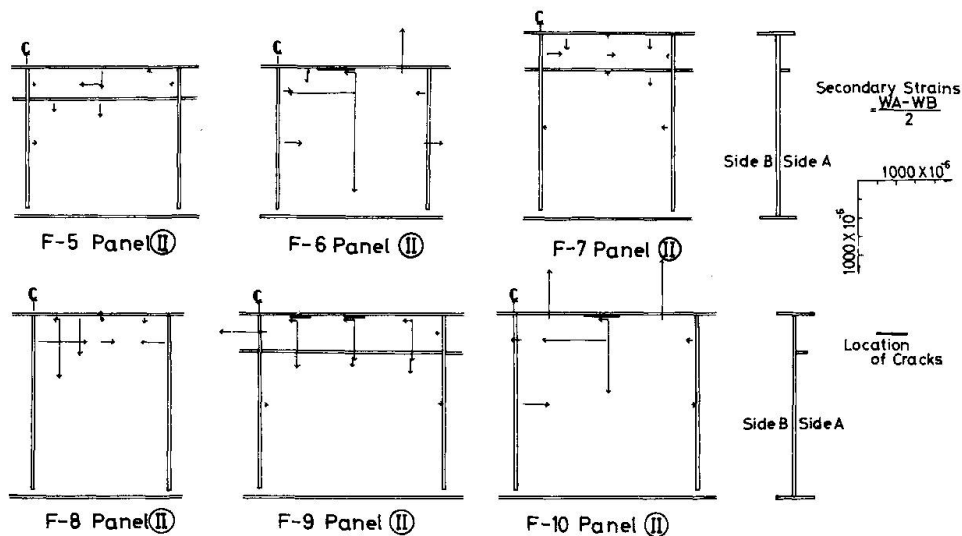


Fig. 16. Secondary Bending Strains due to Web Deflections.

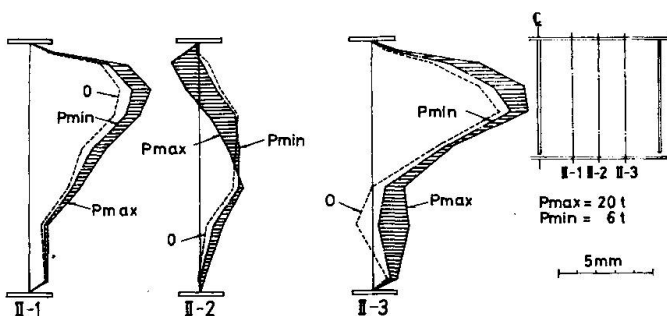


Fig. 18. Lateral Deflections of Web of Girder F-6.

shows that the secondary bending strains due to web deflections influence greatly on the crack initiation. Fig. 17 and Fig. 18 show the lateral deflection of web at zero number of cycles of loads for the girders F-5 and F-6, respectively. Fig. 19 indicates variation of web deflections at zero and 150×10^4 numbers of cycles of loads for the girder F-3.

(3) Effects of slenderness ratio, aspect ratio and longitudinal stiffeners

1) Effect of slenderness ratio of web b/t .

As mentioned before, all of the cracks found in the region of pure bending including the test panels, are of Type BM-1. The relation of crack numbers with

was also shown by the report of Yen and Mueller⁸⁾ that there would be a certain interaction between secondary stresses at web boundaries due to the lateral deflection and the number of cycles of loads at the time of crack initiation.

At the present study, the interaction is not recognized clearly because of rather small numbers of measurement points for web strains near possible locations of the crack initiation, but Fig. 16

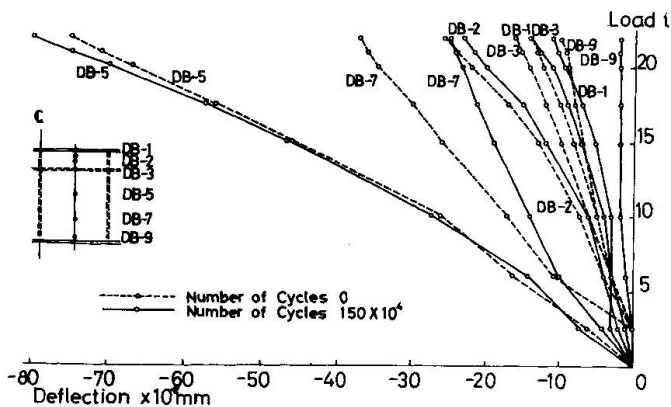


Fig. 19. Variation of Web Deflections for Girder F-3.

Table 8. Effects of b/t , a/b and Longitudinal Stiffener

Test Girder	F-A	F-B	F-1	F-2	F-3	F-4	F-5	F-6
b/t	250		250		300		300	
a/b	0.5	0.5	1.0	1.0	0.75	0.75	1.0	1.0
Longi. Stiffener	1	1	1	0	1	0	1	0
No. of Cracks	0	0	0	3	0	2	5	3
no. of Cycles at Discovery of 1st Crack ($\times 10^4$)	-	-	-	40.5	-	56.6	54.6	12.7

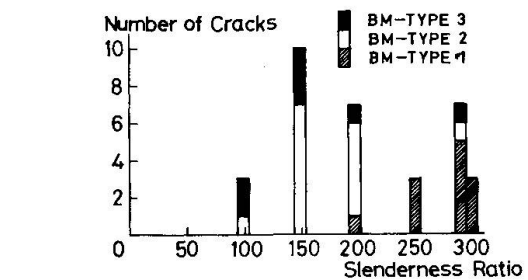


Fig. 20. Number of Cracks versus Slenderness Ratios.

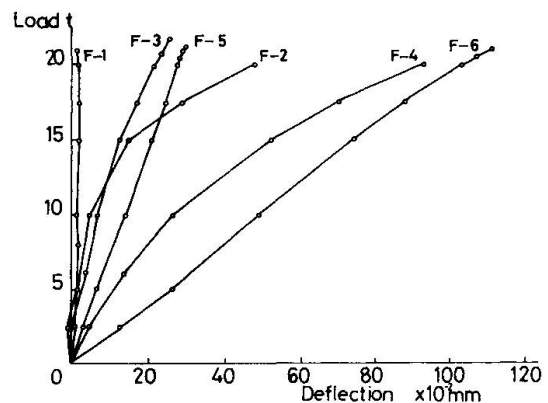


Fig. 21. Web Deflections versus Loads.

slenderness ratio for each type of cracks is illustrated in Fig. 20, from the test results obtained at the author's past and present studies and Toprac's studies^{9),10)}, in which the test data are limited to those of the girders with no longitudinal stiffener and with aspect ratio a/b of 1.0, because they are intended to know the effects of only slenderness ratio. It will be evident from Fig. 20 that the cracks Type BM-1 occurs for girders with the slenderness ratio larger than about 200.

2) Effects of aspect ratio a/b and longitudinal stiffener.

By comparing web deflections of Girders F-1, -3 and -5, with those of Girders F-2, -4 and -6, respectively, it will be noticed that a longitudinal stiffener in the test panel is very effective on restraining the web deflections near the compression flange, which have a close relation with the initiation of cracks. Similarly, by comparing web deflections of Girders F-3 and F-4 with those of Girders F-5 and F-6, respectively, it can be said that a smaller aspect ratio restrains the web deflections. Fig. 21 illustrates variation of web deflections at the point of $0.1b$ from the upper edge of web in the test panel for the girders.

The effect of aspect ratio and longitudinal stiffener will be seen clearly in restraining from the secondary bending strains of web as indicated in Fig. 16, and in reducing the flexural compressive strains in the flange. Girders F-5, however, shows rather large web deflections and secondary bending strains, because the rigidity of its longitudinal stiffeners seem to be relatively smaller. It is shown in Table 8 including the author's previous study results on Girder F-A and F-B, that the aspect ratio and longitudinal stiffeners are related closely with the number of cracks Type BM-1. With the same reason as mentioned above, the number of cracks at F-5 is rather larger. In Girders F-2, -4 and -6, the cracks were found on the both side of web, but those in F-5 did not propagate to the back side

through the web, because of stiffening by the longitudinal stiffeners.

IV. CONCLUSIONS

When the test panels stiffened by transverse and / or longitudinal stiffeners of thin-walled deep plate girders, are subjected to static pure bending or dynamic repeated pure bending, the behavior of web and its influence on the ultimate strength or on the initiation of fatigue cracks have been examined at the present experimental study. The test results will be concluded as follows:

- (1) The test girders which have some hybrid features, showed a similar static behavior to non-hybrid girders, except a rather fast progress of collapse toward their ultimate strength.
- (2) The linear buckling could not be observed due to initial deflections of web, but, with $0.3 t \sim 1.6 t$ in the maximum, they do not seem to have influenced greatly upon the overall ultimate collapse load. In the fatigue tests, however, they influence greatly on the initiation of fatigue cracks Type BM-1 due to the lateral deflections of web in cyclic loadings. The cracks Type BM-1 will be initiated for a plate girder larger than 200 in its web slenderness ratio.
- (3) The single, double-sided or one-sided longitudinal stiffener welded to transverse stiffeners influence greatly on a decrease of lateral deflections of web, patterns of stress distribution over a cross section and an increase of ultimate strength, while it will be subjected to a compressive force. The fatigue tests revealed that it would be possible to prevent the cracks Type BM-1 by providing with longitudinal stiffener, together with a smaller aspect ratio. Rigidities of the longitudinal stiffener were selected to be $3.65 \sim 4.72$ for the static tests and $3.83 \sim 5.30$ for the fatigue tests in terms of relative flexural rigidity δ / δ^* , and a larger ultimate strength, possibly a full-plastic strength could be achieved and an improved fatigue behavior toward prevention of cracks Type BM-1, with a greater rigidity of the longitudinal stiffeners, will be expected.
- (4) For the girders stiffened by a longitudinal stiffener, the reduction of effective width at the ultimate load was observed remarkably in case of $b/t = 250$ and 300, followed by redistribution of web stresses to the compression flange and to the longitudinal stiffeners, where the effective width reduced to $29 \sim 43\%$ of the total depth of web.
- (5) For the longitudinally stiffened girders, Y - shaped compression flanges are more effective than T - shaped flanges in terms of ultimate load, and the former's failure will be governed by lateral buckling and the latter's failure by lateral and/ or torsional buckling. The given width versus thickness ratio of the compression flange did not prevent it from local buckling in plastic range of the stress in the compression flange.

The further experimental studies on large - size hybrid plate girders stiffened by longitudinally stiffeners are being carried out at Osaka University, to obtain more informations for the design of thin-walled deep plate girders.

References

- 1) Y. Maeda and Y. Kubo, "Experimental Study on Ultimate Strength of Longitudinally Stiffened Plate Girders in Bending", 23rd Annual Conference of Japan Society of Civil Engineers, Oct. 1968 (in Japanese).
- 2) K. Basler and B. Thürlimann, "Strength of Plate Girders in Bending", Proc. ASCE, ST 6, 1961.
- 3) H. S. Lew and A. A. Toprac, "Static Strength of Hybrid Plate Girders", S. F. R. L. Tech. Rept. P550 - 11, The University of Texas, Jan. 1968.
- 4) G. Haaijer and B. Thürlimann, "On Inelastic Buckling in Steel", Proc. ASCE, EM 2, 1958.
- 5) American Welding Society, "Article 407. Dimensional Tolerances", Specifications for Welded Highway and Railway Bridges, 1966.
- 6) A. A. Toprac, "Fatigue Strength of Full-Size Hybrid Girders", Proc. AISC National Eng. Conference, 1963.
- 7) T. R. Gurney, "Investigation into the Fatigue Strength of Welded Beams", Part III, British Welding J., Sept. 1962.
- 8) B. T. Yen and J. A. Mueller, "Fatigue Tests of Large-Size Welded Plate Girders", Welding Research Council, Bulletin 118, Nov. 1966.
- 9) H. S. Lew and A. A. Toprac, "Fatigue Tests of Welded Hybrid Plate Girders under Constant Moment", Research Rept. No. 77-2F, Center for Highway Research, The Univ. of Texas, Austin, Jan. 1967.
- 10) Y. Kurobane, D. J. Fielding and A. A. Toprac, "Additional Fatigue Tests of Hybrid Plate Girders under Pure Bending Moment", Res. Rept. No. 96-1F, Center for Highway Research, The Univ. of Texas, Austin, May, 1967.